Eur. Phys. J. B **3**, 17–22 (1998)

THE EUROPEAN PHYSICAL JOURNAL B

Dynamical spin and charge response functions in the doped two-dimensional Hubbard model

T. Saikawa[a] and A. Ferraz

Centro Internacional de Física da Matéria Condensada - ICCMP, Universidade de Brasília, CEP 70919-970 Brasília-DF, Brazil

Received: 25 September 1997 / Revised: 19 December 1997 / Accepted: 9 January 1998

Abstract. Dynamical properties of the spin and charge response functions in the doped two-dimensional Hubbard model are calculated by taking into account the drastic separation of the single-particle spectral function into the low-energy coherent and high-energy incoherent parts due to the strong Coulomb interaction. We show that this evolution of the electronic states is the origin of the broad and structureless feature in the charge response function. In the weak coupling regime the low-energy enhancement of the spin excitation is produced which can be explained within the random phase approximation. However, for the larger interaction close to the antiferromagnetic Stoner condition, the low-energy intensity of the spin excitation is suppressed.

PACS. 71.27.+a Strongly correlated electron systems; heavy fermions – 75.40.Gb Dynamic properties (dynamic susceptibility, spin waves, spin diffusion, dynamic scaling, *etc.*) – 71.10.Fd Lattice fermion models (Hubbard model, *etc.*)

1 Introduction

Spin-gap phenomena which have been observed experimentally in high-temperature superconductors [1–3] and also in non-copper two-dimensional Mott systems [3] is a current issue of the studies in the strongly correlated electron systems. These phenomena seem to be closely related to the mechanism of the high-T_c superconductivity and also to the anomalous metallic phase seen in these materials. Furthermore the possibility of the spin-charge separation in the two-dimensional system [4–7] is also another attractive issue. In spite of its importance, our knowledge on the dynamical properties of the response functions in the strongly correlated electron systems is still limited.

In general, the response of a physical system to an external probe largely depends on the nature of the electronic states in the system. As it is known well, in the Hubbard model, the electronic states suffer dramatic changes due to the on-site Coulomb interaction which appear as evolution of the single-particle spectral function and the density of states. We can summarize their known features [8–11] in three different parameter regimes which can be roughly distinguished by the relative magnitude of the Coulomb interaction U to the non-interacting band width W_0. (i) In the weak-coupling regime ($0 < U \ll W_0$), a weak incoherent background comes out as broadenings of the spectral function in both negative and positive high energy regions. (ii) In the intermediate-coupling regime ($0 \ll U < W_0$), a separation of the high-energy incoherent part and the low-energy coherent part makes progress and this becomes more and more remarkable as U increases. This coherent-incoherent separation in the spectral function causes a band narrowing around the Fermi surface and the evolution of the lower and upper Hubbard bands. Besides it also produces pseudo-gap structures around the narrow quasi-particle band. (iii) In the strong-coupling regime ($U > W_0$), the pseudo-gap becomes larger and if the system is at half-filling, the metal-insulator transition must take place in any space dimension. Thus, in order to study the dynamical properties of the response functions in the strongly correlated electron system, we need to use an approach which describes these modifications of the electronic states.

In our previous work [11] the electronic states of the Hubbard model were investigated numerically using an auxiliary boson approach which combines non-perturbative and perturbative aspects and which considers the effects of both the spin and charge fluctuations. In the calculation the fermion-boson interactions were taken into account up to the one-loop level in the boson and fermion self-energies. In our previous paper using this scheme we have obtained the above mentioned evolution of the electronic states from the weak-coupling up to the intermediate-coupling regime which is controlled by a Stoner condition. The obtained behavior of the electronic states are in good agreement with the results of the numerical simulations [8,9]. In this paper, using the same scheme, we investigate the behavior of the spin and charge response functions in the two-dimensional Hubbard model as we vary

[a] e-mail: saikawa@iccmp.br

the Coulomb interaction U in the paramagnetic regime. We focus on how the dynamical properties of the spin and charge response functions are affected by the drastic changes in the electronic states.

2 Model and spectral function

In this section, following our previous work [11] we introduce an auxiliary boson approach to describe the electronic states of the Hubbard model. At first, we briefly review how to derive the Green's function in our scheme including one-loop fermion self-energy effect due to the boson fluctuations. More detailed derivation of the fermion Green's function and detailed analysis of the electronic states derived by our approach have been given in reference [11].

We start with the following Hubbard Hamiltonian in the two-dimensional square lattice,

$$H = -t \sum_{\langle i,j\rangle,\sigma} c^{\dagger}_{i\sigma} c_{j\sigma} + U \sum_{i} n_{i\uparrow} n_{i\downarrow} - \mu \sum_{i,\sigma} n_{i\sigma}. \quad (1)$$

The notation is standard and in the first term only the nearest-neighbor hopping t is considered. Here, μ is the chemical potential. The Lagrangian density of this model can be written as

$$\begin{aligned}\mathcal{L} = &\sum_{\sigma} \Psi^{\dagger}_{\sigma}(\mathbf{r},t)(i\partial_t + \mu)\Psi_{\sigma}(\mathbf{r},t) \\ &+ t \sum_{j=x,y} \sum_{\sigma} \Psi^{\dagger}_{\sigma}(\mathbf{r},t)\Psi_{\sigma}(\mathbf{r} \pm \mathbf{e}_j, t) \\ &- \frac{U}{2} \sum_{a,b=0}^{3} \rho^{(a)}(\mathbf{r},t)\eta_{ab}\rho^{(b)}(\mathbf{r},t) \end{aligned} \quad (2)$$

where $\Psi^{\dagger}, \Psi$ are Grassmann fields, $\mathbf{e}_j$ is the unit lattice vector for j direction on the lattice space, and η_{ab} denotes the element of a diagonal matrix which has diagonal elements $\eta_{00} = 1$ and $\eta_{11} = \eta_{22} = \eta_{33} = -1$, and we have rewritten the interaction term in equation (1) using one charge ($a = 0$) and three spin ($a = 1, 2, 3$) density operators defined by

$$\rho^{(a)}(\mathbf{r},t) = \frac{1}{2} \sum_{\sigma,\sigma'} \Psi^{\dagger}_{\sigma}(\mathbf{r},t)\tau^{(a)}_{\sigma\sigma'}\Psi_{\sigma'}(\mathbf{r},t) \quad (3)$$

with the Pauli matrices

$$\tau^{(1)} = \begin{bmatrix} 0 & 1 \\ 1 & 0 \end{bmatrix}, \tau^{(2)} = \begin{bmatrix} 0 & -i \\ i & 0 \end{bmatrix}, \tau^{(3)} = \begin{bmatrix} 1 & 0 \\ 0 & -1 \end{bmatrix} \quad (4)$$

and the 2×2 unit matrix

$$\tau^{(0)} = \begin{bmatrix} 1 & 0 \\ 0 & 1 \end{bmatrix}. \quad (5)$$

Next, we introduce four auxiliary bosonic operators $\phi^{(a)}(\mathbf{r},t)$ for one charge- and three spin-density operators by the Hubbard-Stratonovich transformation [11]. Then the Lagrangian density becomes

$$\begin{aligned}\mathcal{L}' = &\sum_{\sigma} \Psi^{\dagger}_{\sigma}(\mathbf{r},t)(i\partial_t + \mu)\Psi_{\sigma}(\mathbf{r},t) \\ &+ t \sum_{j=x,y} \sum_{\sigma} \Psi^{\dagger}_{\sigma}(\mathbf{r},t)\Psi_{\sigma}(\mathbf{r} \pm \mathbf{e}_j, t) \\ &+ \frac{\sqrt{U}}{2} \sum_{\sigma,\sigma'} \sum_{a,b} \eta_{ab}\phi^{(a)}(\mathbf{r},t)\Psi^{\dagger}_{\sigma}(\mathbf{r},t)\tau^{(b)}_{\sigma\sigma'}\Psi_{\sigma'}(\mathbf{r},t) \\ &+ \frac{1}{2} \sum_{a,b} \phi^{(a)}(\mathbf{r},t)\eta_{ab}\phi^{(b)}(\mathbf{r},t). \end{aligned} \quad (6)$$

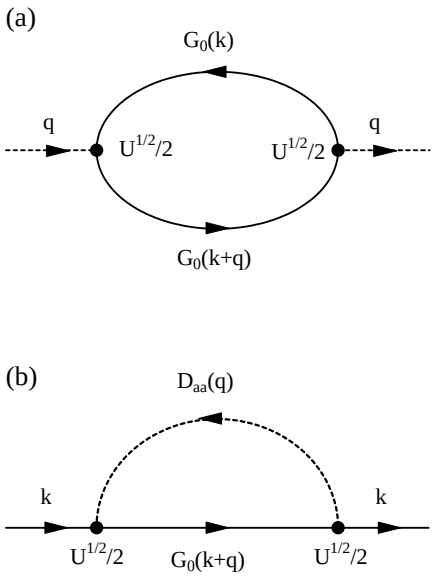

Fig. 1. Diagram representations of (a) the polarization function $\chi_0(q)$ and (b) the fermion self-energy $\Sigma_a(k)$.

In order to give true physical meaning to the bosonic modes we integrate out the Grassmann fields and obtain an effective action for the boson fields [11]. By introducing the boson fluctuation with $\phi^{(a)} = \phi^{(a)}_0 + \delta\phi^{(a)}$ where $\phi^{(a)}_0$ denotes the saddle point solution of the effective action, we can expand this action around the saddle point. Taking into account boson fluctuation effects up to the quadratic term, we obtain the boson propagator written by [11]

$$D_{aa}(q) = \frac{1}{\eta_{aa} + (U/2)\chi_0(q)} \quad (7)$$

with $q = (\mathbf{q}, \omega_b)$. Since we consider the paramagnetic states, the three spin components of the boson propagator are equivalent each other. The polarization function $\chi_0(q)$ is given by

$$\chi_0(q) = i \int_k G_0(k+q)G_0(k) \quad (8)$$

with $k = (\mathbf{k}, \omega)$ and we use the abbreviation $\int_k = \int \frac{d\omega}{2\pi} \frac{d\mathbf{k}}{(2\pi)^2}$. $G_0(k)$ is the mean-field Green's function defined with the mean-field energy band $E_{\mathbf{k}} = \varepsilon_{\mathbf{k}} - \mu_0$.

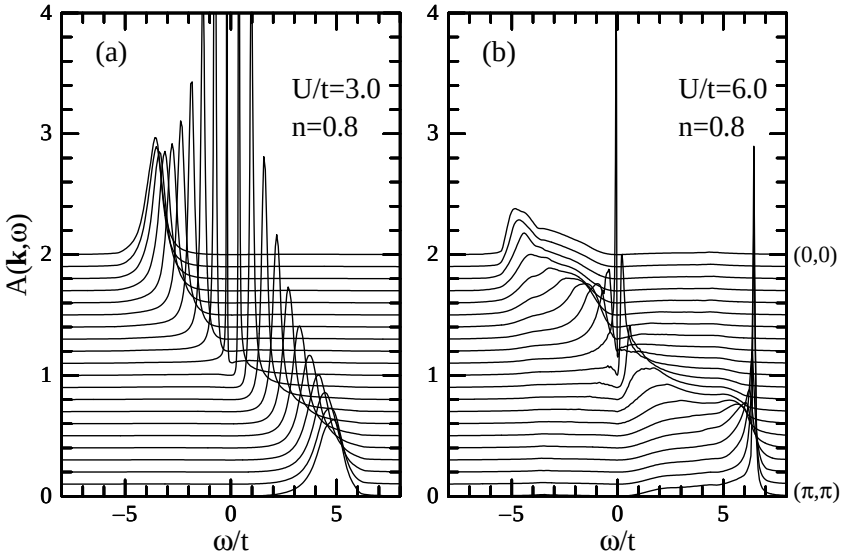

Fig. 2. Spectral functions $A(k), k = (\mathbf{k}, \omega)$ for the $(1,1)$ direction calculated at $n = 0.8$, for (a) $U/t = 3.0$ and (b) 6.0. Each spectral function is shifted and the top (bottom) corresponds to $\mathbf{k} = (0,0)$ ($\mathbf{k} = (\pi, \pi)$).

$\varepsilon_{\mathbf{k}} = -2t(\cos k_x + \cos k_y)$ is the tight-binding band dispersion in the two-dimensional square lattice and μ_0 is the mean-field chemical potential that contains a Hartree-Fock energy and it can be determined to satisfy the electron number conservation relation. The diagrammatic representation of $\chi_0(q)$ is shown in Figure 1a. Note that the denominator of the spin boson propagator gives the Stoner criterion $1 - (U/2)\mathrm{Re}(\chi_0(\mathbf{q}, 0)) = 0$.

To go beyond this mean-field approximation we consider a model consisting of the boson free term and of the fermion fields. The free boson term is given by the above mentioned non-perturbatively derived boson propagator D_{aa}. The boson and fermion fields are interacting with through an interaction term such as the third term of equation (6). The full effective action of this model [12] can be written as

$$\begin{aligned} S_{eff} = &\sum_{\sigma} \int_k \tilde{\Psi}^{\dagger}_{\sigma}(k)(\omega + \mu - \varepsilon_{\mathbf{k}})\tilde{\Psi}_{\sigma}(k) \\ &+ \sum_{a=0}^{3} \int_q \frac{1}{2} \delta\tilde{\phi}^{(a)}(-q) D_{aa}(q)^{-1} \delta\tilde{\phi}^{(a)}(q) \\ &+ \sum_{a=0}^{3} \sum_{\sigma,\sigma'} \int_k \int_q \delta\tilde{\phi}^{(a)}(q) \frac{\sqrt{U}}{2} \eta_{aa} \tilde{\Psi}^{\dagger}_{\sigma}(k+q) \tau^{(a)}_{\sigma\sigma'} \tilde{\Psi}_{\sigma'}(k) \end{aligned} \tag{9}$$

where the symbols with tilde represent the Fourier transformed fields. The fermion-boson coupling in this effective model generates non-trivial self-energy effects. In fact, up to the one-loop order, the fermion self-energy for both the charge and spin components can be written as

$$\Sigma_a(k) = i\frac{U}{4} \int_q G_0(k+q) D_{aa}(q). \tag{10}$$

The corresponding diagram is shown in Figure 1b. In this way, we obtain the dressed fermion Green's function given by

$$G(k)^{-1} = \omega + \mu_* - \varepsilon_{\mathbf{k}} - \sum_{a=0}^{3} \Sigma_a(k) \tag{11}$$

where the chemical potential μ_* can be determined consistently with a fixed electron concentration n. The spectral function can be defined by $A(k) = -(1/\pi)\mathrm{sgn}(\omega)\mathrm{Im}(G(k))$.

In Figure 2, we show the evolution of the spectral function which has been calculated in our previous work [11]. It can be observed that as the interaction U increases, the spectral function suffers an essential change, namely the separation between the low-energy sharp coherent part around the Fermi energy ($\omega/t = 0$) and the high-energy broad incoherent parts. The broadenings of the spectral function can be produced by the self-energy effect. Note that the energy dependence of the spectral function at the momentum neighboring but not on the Fermi surface is rather incoherent in the low energy region. Such incoherent spectral functions have been observed in a number of experimental data of the angle-resolved photoemission spectroscopy for high-T_c materials [13].

3 Spin and charge response functions

In this section we investigate how the coherent and incoherent natures in the single-particle spectral function affect the behavior of the energy dependence of the response functions by varying the value of the coupling constant U. We define the retarded spin (χ_s) and charge (χ_c) response functions [14] as

$$\chi_s(\mathbf{q}, t-t') = i\theta(t-t') \left\langle [m^{(z)}_{\mathbf{q}}(t), m^{(z)}_{-\mathbf{q}}(t')] \right\rangle, \tag{12}$$

$$\chi_c(\mathbf{q}, t-t') = i\theta(t-t') \langle [n_{\mathbf{q}}(t), n_{-\mathbf{q}}(t')] \rangle \tag{13}$$

where $m_{\mathbf{q}}^{(z)}(t)$ and $n_{\mathbf{q}}(t)$ are the Fourier components of the spin and charge density operator defined by

$$m^{(z)}(\mathbf{r},t) = \sum_{\sigma} \sigma \Psi_{\sigma}^{\dagger}(\mathbf{r},t)\Psi_{\sigma}(\mathbf{r},t),$$
$$n(\mathbf{r},t) = \sum_{\sigma} \Psi_{\sigma}^{\dagger}(\mathbf{r},t)\Psi_{\sigma}(\mathbf{r},t), \quad (14)$$

respectively. Using the fermion-boson effective action given by equation (9), the expansion series of the response functions can be derived. In this diagrammatic expansion, one needs to avoid the double counting of the polarization function χ_0 which has already been taken into account in the boson propagators. From this expansion we make a partial summation consisting of the terms that have no vertex corrections in any diagrams. Then, the spin ($\alpha = s$) and charge ($\alpha = c$) response functions can be written as

$$\chi_{\alpha}(q) = \frac{2\Pi(q)}{1 + \eta_{\alpha}\frac{U}{2}\Pi(q)} \quad (15)$$

where $\eta_s = -1$, $\eta_c = 1$ and the polarization function $\Pi(q)$ is defined by

$$\Pi(q) = i\int_k G(k+q)G(k) \quad (16)$$

using the *dressed* fermion Green's function $G(k)$ given by equation (11). The spectrum of the spin ($\alpha = s$) and charge ($\alpha = c$) response functions is defined by the imaginary part of $\chi_{\alpha}(q)$ as

$$\mathrm{Im}(\chi_{\alpha}(q)) = \frac{2\mathrm{Im}(\Pi(q))}{\left(1 + \eta_{\alpha}\frac{U}{2}\mathrm{Re}(\Pi(q))\right)^2 + \left(\frac{U}{2}\mathrm{Im}(\Pi(q))\right)^2} \quad (17)$$

with

$$\mathrm{Im}(\Pi(q)) = \int_k [1 - \mathrm{sgn}(\omega+\omega_b)\mathrm{sgn}(\omega)] \times \mathrm{Im}(G(k+q))\mathrm{Im}(G(k)) \quad (18)$$

and $\mathrm{Re}(\Pi(q))$ being calculated from $\mathrm{Im}(\Pi(q))$ by applying the Kramers-Kronig relation [15].

Using these formulae and also the dressed Green's function $G(k)$, we performed numerical calculations of the polarization function and also of the spin and charge response functions for some values of U. The choice of the coupling constant is still restricted due to the Stoner criterion which works in the boson propagator $D_{aa}(q)$.

Figure 3 shows the U evolution of the polarization function $\mathrm{Im}(\Pi(q))$ at the electron concentration $n = 0.8$ for several wave vector $\mathbf{q}$'s in the (1,1) direction. For $U/t = 0$, $\mathrm{Im}(\Pi(q)) = \mathrm{Im}(\chi_0(q))$ which has a specific structure at each $\mathbf{q}$. The shape of $\mathrm{Im}(\chi_0(q))$ is completely dominated by the non-interacting band structure. As U increases, the overall structure of $\mathrm{Im}(\Pi(q))$ becomes broader and structureless at each $\mathbf{q}$. Besides, the intensity of $\mathrm{Im}(\Pi(q))$ is reduced remarkably in low energy region around $\omega_b/t \sim 1$.

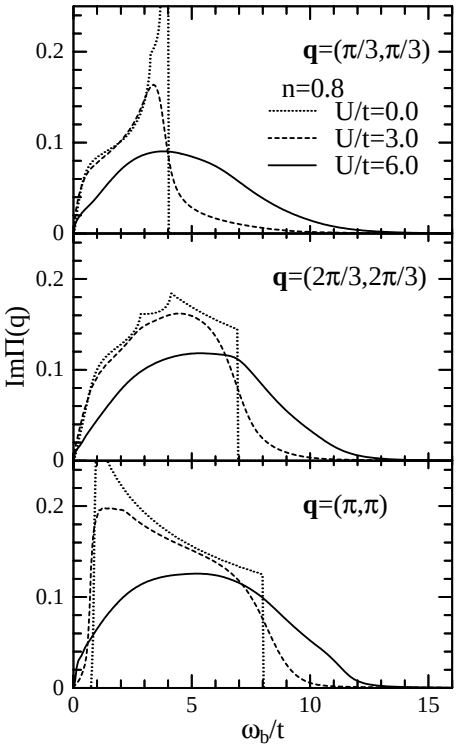

Fig. 3. Energy dependence of the polarization function $\mathrm{Im}(\Pi(q))$ for $U/t = 0.0$ (dotted line), 3.0 (dashed line), 6.0 (solid line) at $n = 0.8$ and for several wave vector $\mathbf{q}$'s.

These features in $\mathrm{Im}(\chi_0(q))$ can be understood by analyzing the dressed Green's function. We consider to separate the dressed Green's function $G(k)$ into the coherent quasiparticle Green's function $g(k)$ and the incoherent Green's function $G_{inc}(k)$. The phenomenological quasiparticle concept may have been established and known well since the Landau's work on the Fermi-liquid. But, we don't have exact ways to distinguish only the quasiparticle states from the total electronic states without doing any approximations. Here, without describing a prescription to extract the quasiparticle Green's function from the full Green's function, we simply write down the full Green's function $G(k)$ as the sum of the coherent and incoherent parts as

$$G(k) = g(k) + G_{inc}(k). \quad (19)$$

We assume that $g(k)$ has been extracted from $G(k)$ in terms of an approximation capturing the phenomenological properties of the quasiparticle and we define the incoherent part by $G_{inc}(k) = G(k) - g(k)$. By making this split, $\mathrm{Im}(\Pi(q))$ can be written as

$$\mathrm{Im}(\Pi(q)) = \int_k [1 - \mathrm{sgn}(\omega+\omega_b)\mathrm{sgn}(\omega)] \times \{\mathrm{Im}\, g(k+q)\mathrm{Im}\, g(k) + \mathrm{Im}\, g(k+q)\mathrm{Im}\, G_{inc}(k) + \mathrm{Im}\, G_{inc}(k+q)\mathrm{Im}\, g(k) + \mathrm{Im}\, G_{inc}(k+q)\mathrm{Im}\, G_{inc}(k)\}. \quad (20)$$

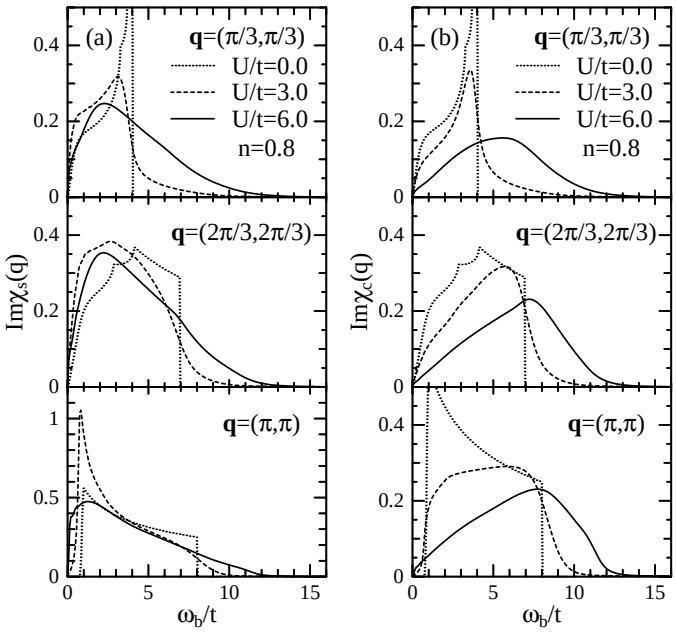

Fig. 4. Energy dependence of (a) the spin response function $\mathrm{Im}(\chi_s(q))$ and (b) the charge response function $\mathrm{Im}(\chi_c(q))$ for $U/t = 0.0$ (dotted line), 3.0 (dashed line), 6.0 (solid line) at $n = 0.8$ and for several wave vector $\mathbf{q}$'s. Note that only the case $\mathbf{q} = (\pi, \pi)$ in (a) was plotted in a different scale.

The condition $\mathrm{sgn}(\omega + \omega_b)\mathrm{sgn}(\omega) - 1 \neq 0$ in the integrand gives a restriction in the range of the integral over ω. If $\omega_b > 0$, it follows that $0 < \omega_b + \omega < \omega_b$ and $-\omega_b < \omega < 0$. Because of these conditions, for small ω_b, the main contribution comes from the first term consisting of a convolution of the two quasiparticle Green's functions. On the other hand, contribution to the high ω_b region comes from the incoherent part $\mathrm{Im}(G_{inc}(k))$ of the spectral function. Even if the quasiparticle spectrum has some intensity, the integrated intensity of the first term of $\mathrm{Im}(\Pi(q))$ becomes small because the total weight of the quasiparticle spectrum becomes smaller as U increases. Thus as U becomes large, the intensity of the low energy part of $\mathrm{Im}(\Pi(q))$ decreases.

In Figure 4a the spin response function $\mathrm{Im}(\chi_s(q))$ is shown for different U's. For $U/t = 3.0$, the spin response function has a low energy enhancement at $\mathbf{q} = (\pi, \pi)$. This is the Stoner enhancement (antiferromagnetic paramagnon) which can be explained by RPA. For $U/t = 6.0$, the low energy intensity decreases because of the above mentioned decrease of intensity in the polarization function. This can be interpreted as the damping of the antiferromagnetic paramagnon. The main weight of $\mathrm{Im}(\chi_s(q))$ moves to a low energy region for every $\mathbf{q}$. Besides, in the high energy region the spin response function has a long tail. In Figure 4b the charge response function $\mathrm{Im}(\chi_c(q))$ is plotted in the same way as shown in Figure 4a. As U becomes large, the charge response function becomes structureless and broader. Contrary to the behavior of the spin response function, the main weight of the charge response function shifts to the high energy region.

4 Discussion

In some theoretical and simulation based studies, the dynamical spin and charge response functions have already been calculated for the t-J model [16–19], the $U = \infty$ Hubbard model (t model) [20] and the Hubbard model [9,21–23]. In these works two common specific features of the response functions can be seen: (i) the spin response function has a large peak near the low energy region for sufficiently small dopings, (ii) the charge response function shows highly broad structures over a wide energy range. There is a separation of the energy scale of the spin and charge fluctuations which is consistent with our results. In our scheme such energy scale separation in the response functions is strongly coupled with the incoherent-coherent separation in the electronic states. Our approach gives a non-trivial qualitatively correct description and the results for the spectral functions and also for the dynamical properties of the response functions agree qualitatively well with the simulation results.

We compare our result with a different calculation taking into account the spin-fluctuation effects [22]. They found the sharp peak of $\mathrm{Im}(\chi_s(q))$ at $\mathbf{q} = (\pi, \pi)$, for $U/t = 1.0$ (in our definition) and at a suitable doping where the Fermi energy is located at the larger intensity sector of the density of states in their calculation. They explained this effects by the Pauli-susceptibility and the large intensity of the density of states near the Fermi energy. This explanation is valid for the small value of U/t in their calculation, because the Stoner enhancement may be small in the weak-coupling regime. The sharp peak at the $\mathbf{q} = (\pi, \pi)$ is also observed in our numerical result. However its origin is explained by the Stoner enhancement in our case as we have mentioned in the previous section. A similar result to ours has already been obtained in the calculation with the FLEX approximation for $U/t = 4.0$ and at sufficiently small doping ($n = 0.96$) [21], and for $U/t = 4.3$ and at $n = 0.831$ but for $\mathbf{q}/\pi = (1.0, 0.844)$ [23]. These results can be understood as a manifestation of the collective mode associated with the Stoner enhancement. The same trend can be seen in the calculation based on a slave-boson-like approach for the $U = \infty$ Hubbard model [20]. However, the enhancement of the electronic density of states coming from the band narrowing effect seems to be the major effect of the sharp peak of the spin excitation in their calculation.

The Stoner criterion is an important restriction in our approximation. We can't apply the present treatment for larger values of U beyond this limit. Our treatment is suitable in the paramagnetic regime, but it is not appropriate, for instance, in antiferromagnetic regime. This Stoner criterion is however strongly dependent on the kind of approximation one takes into account. If we extend our approach into a suitable self-consistent calculation or consider further vertex corrections, the limitation imposed by the Stoner criterion becomes looser and the calculation in the large coupling region and at the smaller dopings may become accessible to us. One different method, the fluctuation exchange (FLEX) approximation [21,23, 24], takes some account of self-consistency with no vertex

correction. However, the FLEX approximation and our approach show basically the same physical trends.

In summary, we have investigated dynamical properties of the polarization function and also the spin and charge response functions by taking into account the single-particle spectral functions which include one-loop boson and fermion self-energy effects. The striking evolution of the spectral function due to the Coulomb interaction produces structureless broad features over a wide energy range in the polarization function. The spin and charge response functions have been calculated with this polarization function. In the weak-coupling regime, the low energy excitation manifests itself in the spin response function. This can be explained by the standard RPA approximation. However, as U becomes larger beyond the weak-coupling regime, the low energy enhancement in the spin response function decreases and in the high energy region it shows a long tail. The charge response function becomes broader monotonically as U becomes larger. These behaviors in both the spin and charge response functions cannot be explained within the standard RPA and it is a clear manifestation of the drastic changes in the nature of the single-particle electronic states at large values of U. We emphasize that the dynamical properties of the response functions are strongly correlated with the drastic change of the spectral functions. Our approach explains this feature qualitatively well.

We would like to acknowledge useful discussions with H. Kaga, S.L. Garavelli, X. Xue, P.E. de Brito, and S. Gluzman. This work was supported by the Conselho Nacional de Desenvolvimento Científico e Tecnológico - CNPq and by the Financiadora de Estudos e Projetos - FINEP. The numerical calculations were performed in the supercomputing system at the Institute for Materials Research, Tohoku University, Japan.

References

1. H. Yasuoka, T. Imai, T. Shimizu, in *Strong Correlation and Superconductivity*, edited by H. Fukuyama, S. Maekawa, A.P. Malaozemoff (Springer-Verlag, Berlin, 1989).
2. J. Rossat-Mignod *et al.*, Physica B **163**, 4 (1990).
3. M. Sato, Physica C **263**, 271 (1996); and references therein.
4. Y. Suzumura, Y. Hasegawa, H. Fukuyama, J. Phys. Soc. Jpn **57**, 2768 (1988).
5. H. Fukuyama, Physica C **263**, 35 (1996).
6. W.O. Putikka, R.L. Glenister, R.R.P. Singh, H. Tsunetsugu, Phys. Rev. Lett. **73**, 170 (1994).
7. Y.C. Chen, A. Moreo, F. Ortolani, E. Dagotto, T.K. Lee, Phys. Rev. B **50**, 655 (1994).
8. E. Dagotto, Rev. Mod. Phys. **66**, 763 (1994); and references therein.
9. R. Preuss, W. Hanke, C. Gröber, H.G. Evertz, Phys. Rev. Lett. **79**, 1122 (1997).
10. H. Matsumoto, F. Mancini, Phys. Rev. B **55**, 2095 (1997).
11. T. Saikawa, A. Ferraz, P.E. de Brito, H. Kaga, Phys. Rev. B **56**, 4464 (1997).
12. Note that this effective model is equivalent with the original Hubbard model if we properly consider the double counting of the polarization function χ_0 in the boson propagators when we perform a diagrammatic expansion. This feature was taken into account in our calculation of the response functions (see Sect. 3).
13. Z.-X. Shen, D.S. Dessau, Phys. Rep. **253**, 1 (1995), see also references therein; H. Ding, *et al.*, Phys. Rev. Lett. **76**, 1533 (1996).
14. See for example, S. Doniach, E.H. Sondheimer, *Green's Functions for Solid State Physicists*, (Addison - Wesley, New York, 1974).
15. See for example, A.A. Abrikosov, L.P. Gorkov, I.E. Dzyaloshinski, *Methods of Quantum Field Theory in Statistical Physics* (Dover, New York, 1963).
16. T. Tohyama, P. Horsh, S. Maekawa, Physica C **235−240**, 2231 (1994); Phys. Rev. Lett. **74**, 980 (1995).
17. R. Eder, Y. Ohta, S. Maekawa, Phys. Rev. Lett. **74**, 5124 (1995).
18. D.K.K. Lee, D.H. Kim, P.A. Lee, Phys. Rev. Lett. **76**, 4801 (1996).
19. G. Khaliullin, P. Horsch, Phys. Rev. B **54**, R9600 (1996).
20. L. Gehlhoff, R. Zeyher, Phys. Rev. B **52**, 4635 (1995).
21. N.E. Bickers, D.J. Scalapino, S.R. White, Phys. Rev. Lett. **62**, 961 (1989).
22. S. Charfi-Kaddour, R.J. Tarento, M. Heritier, J. Phys. I France **2**, 1853 (1992).
23. T. Dahm, L. Tewordt, Phys. Rev. Lett. **74**, 793 (1995).
24. N.E. Bickers, D.J. Scalapino, Ann. Phys. N.Y. **193**, 206 (1989).